

# Optical conductivity of wet DNA

A. Hübsch<sup>1</sup>, R. G. Endres<sup>2</sup>, D. L. Cox<sup>1,3,4</sup>, and R. R. P. Singh<sup>1,3</sup>

<sup>1</sup>*Department of Physics, University of California, Davis, CA 95616*

<sup>2</sup>*NEC Laboratories America, Inc., Princeton, NJ 08540*

<sup>3</sup>*Center for Biophotonics Science and Technology, University of California, Davis, CA 95616*

<sup>4</sup>*Center for Theoretical Biological Physics, University of California, San Diego, CA 92119*

(Dated: January 25, 2005)

Motivated by recent experiments we have studied the optical conductivity of DNA in its natural environment containing water molecules and counter ions. Our density functional theory calculations (using SIESTA) for four base pair B-DNA with order 250 surrounding water molecules suggest a thermally activated doping of the DNA by water states which generically leads to an electronic contribution to low-frequency absorption. The main contributions to the doping result from water near DNA ends, breaks, or nicks and are thus potentially associated with temporal or structural defects in the DNA.

PACS numbers: 87.14.Gg, 87.15.Aa, 87.15.Mi

*Introduction.* The electronic properties of DNA have received considerable scientific attention in the last few years, motivated both by possible use in molecular electronics [1] and by speculation that electrons can speed up the location (and possibly repair) of damage sites by relevant proteins in living cells [2]. A number of experiments have been carried out to measure the conductance of DNA in different contexts (for a recent review see Ref. 3). Of particular note have been observations of activated behavior with small gaps, of order 0.1-0.3 eV [4, 5], which stand in contrast to the peak optical absorption of DNA in the ultraviolet at 3.5-4 eV. Evidently, such small activation energies, if they are not extrinsically induced, require an intrinsic doping mechanism for the DNA to overcome the large gap.

To address this issue, we have studied several DNA tetramers surrounded by waters and counterions using a combination of classical molecular dynamics (MD) with density functional theory (DFT) employing the local basis set SIESTA code [7]. To our knowledge, this is the first time that the electronic conductivity of DNA has been computed with a full quantum mechanical treatment of water and counter-ions in a dynamically fluctuating environment, although similar methods have been used before to study charge migration in DNA [8, 9] *without* explicit quantum treatment of the environment. Our tetramers are in the fully hydrated biological form (B-DNA), with order 250 water molecules. We find evidence that waters in contact with DNA bases can dope the DNA with excitation gaps as small as 0.1-0.3 eV. Our calculations provide absorption at low frequencies in agreement with optical experiments [5] if we increase the number of bases exposed to water. In a cellular environment, these will be associated with temporal or structural defects, but in many solid-state experiments can also arise from the flattening and unwinding of the DNA helix.

Our calculations also provide insight into the peak absorption in DNA in the ultraviolet at 3.5-4 eV and its variation with sequence and environmental configura-

tions. These polarization dependent absorptions form the basis for well established methods to probe DNA molecules using Circular Dichroism and Optical Rotation [6]. We find that the calculated frequency dependent optical conductivity agrees quantitatively with the measured peak absorption for  $\lambda$ -phage DNA[5]. We also find that, while the peak location is very stable, there are distinct features near the peak, which vary with DNA sequence and different environmental configurations accessed during a typical MD run. Within the time scales of the MD (out to 1 ns), our conductivity calculations are unable to uniquely determine sequence specificity, but some specificity/fingerprinting may be possible with signal averaging.

These results confirm that while the DNA molecule is a large-gap material, environmental conditions can induce states in the gap, which can in turn lead to a small but non-zero sub-gap absorption. Such states are also crucial for understanding room temperature thermally activated electron dynamics in the DNA, a mechanism that has gained wide acceptance for observed electron transfer in DNA over very long ranges [1].

Band structure calculations to study the electronic structure of DNA have been performed for dry A-DNA [10] and for crystallized Z-DNA [11] where the effects of solvent and counterions have also been addressed. Here, we extend our recent work [12] by considering dynamical fluctuations of the environment. Other efforts have been made to study electronic spectra of DNA in fluctuating environments both without [13] and with [8, 9] counterions and water. Our work differs from these latter efforts by the explicit quantum mechanical treatment of water and counterion states.

*Methodology.* To calculate the electronic spectra and optical conductivity we have used the fully ab initio DFT code SIESTA [7]. It uses Troullier-Martins norm-conserving pseudo potentials [14] in the Kleinman-Bylander form [15]. We have used the generalized gradient approximation (GGA) for the exchange-correlation energy functional in the version of Perdew, Burke, and

Ernzerhof [16]. SIESTA uses a basis set of numerical atomic orbitals where the method by Sankey and Niklewski [17] is employed. For the DNA we have used a double- $\zeta$  basis set except for phosphorus, hydrogen involved in hydrogen bonding, and the counterions for which the polarization orbitals have also been included. For the surrounding water molecules (about 250) we have only used the minimal, single- $\zeta$  basis set.

The optical conductivity is given by the Kubo formula

$$\sigma_{1,\mu}(\omega) = \pi \frac{e^2}{V} \frac{1 - e^{-\beta\hbar\omega}}{\omega} \sum_{n,m} \frac{e^{-\beta\varepsilon_n}}{Z} \delta(\varepsilon_n - \varepsilon_m - \hbar\omega) |\langle n | j_\mu | m \rangle|^2$$

and depends on the frequency  $\omega$ . Here,  $\varepsilon_n$ ,  $\varepsilon_m$  and  $|n\rangle$ ,  $|m\rangle$  are the energies and wave functions of the DFT Hamiltonian, respectively.  $V$  denotes the unit cell volume, and  $j_\mu$  with  $\mu = \perp, \parallel$  is the component of the current operator perpendicular or parallel to the DNA strand direction. The conductivity computed here does not include time dependent DFT or scissors corrections.

The solvated DNA structures were obtained from classical MD simulations with the AMBER7 package [18] (parm98 force field). The four base-pair long DNA structures (B-DNA 5'-GAAT-3', 5'-GGGG-3', 5'-AAAA-3', and TT-dimer) were initially charge-neutralized with counterions (either by 6 monovalent sodium or 3 divalent magnesium ions) and solvated with about 600 TIP3P water molecules. A simulation box of dimensions  $38 \times 35.4 \times 25 \text{ \AA}^3$  (z-axis parallel to DNA axis) with periodic boundary conditions was applied. After equilibration at room temperature for 1 ns, the trajectory was recorded every 10 ps over a production simulation time of 1 ns. The resulting 100 snapshots were used for subsequent analysis. All our simulations employed the SHAKE method to fix hydrogen-heavy atom distances allowing a 2 fs integration time step. The cut-off for long-range interactions was set to  $10 \text{ \AA}$ . TT-dimer (segment 5'-ATTA-3' from PDB code 1SM5) was furthermore constrained using the BELLY option to preserve the distorted DNA structure.

To use the structures obtained from the MD simulations for the DFT calculations we had to reduce the number of atoms. Therefore, we have only kept the first and second solvation shell (approximatively 30 water molecules per nucleotide) which means that all water molecules within a  $4.7 \text{ \AA}$  radius have been included in the calculations. Finally, we incorporated about 1000 atoms in our DFT calculation so that the numerical computations were quite time consuming. In particular, the evaluation of the optical conductivity is very expensive. To speed up the computations we restricted the number of included unoccupied states which only affects the high-energy range above 5 eV of the spectra. Thus, the calculation of the optical conductivity for a given structure snapshot took about 5 days on AMD's Opteron CPU where approximatively 2 GB RAM were needed. All cal-

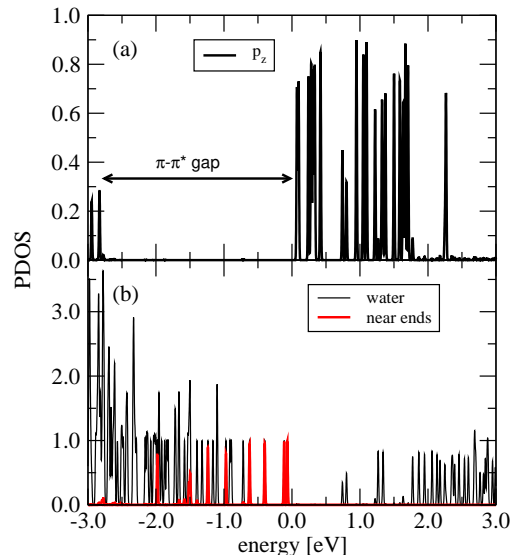


FIG. 1: Typical PDOS of a structure snapshot of a 5'-GAAT-3' sequence with Mg counterions. Panel (a) shows the  $p_z$  orbitals of atoms in base pairs. Panel (b) contains the PDOS of all water molecules (thin black line) where the contributions of water molecules near the sequence ends are plotted by a thick red line. The Fermi energy is set to 0.0 eV.

culations have been carried out at room temperature. To consider the dynamically fluctuating character of the DNA environment we averaged the results of the optical conductivity over up to 9 structure snapshots spread over the MD time scale.

*Results.* In order to identify the energetically important states near the Fermi energy, we projected the density of states (DOS) on the atomic  $p_z$  orbitals of the base pairs and on the water molecules. Note that we also calculated the projected DOS of the counterions, phosphates, and the sugars. However, we only found contributions of the  $p_z$  orbitals and the water molecules near the Fermi level. A typical projected DOS of structure snapshot of a 5'-GAAT-3' sequence with Mg counterions is shown in Fig. 1. As one can see from panel (a), there is a rather large  $\pi-\pi^*$  gap of about 2.7 eV. However, if we project the DOS on a single base we would find an intrabase  $\pi-\pi^*$  gap of about 3.7 eV. It turns out that only such intrabase transitions have large dipole matrix elements. Therefore, we observe optical gaps of the same size (compare Figs. 2 and 3).

Although a rather big  $\pi-\pi^*$  gap is observed the actual gap between the highest occupied molecular orbital (HOMO) and the lowest unoccupied molecular orbital (LUMO) of about 150 meV is very small [combine panels (a) and (b) of Fig. 2]. Thus, electrons could be excited from water states below the Fermi energy into unoccupied  $p_z$  orbitals due to thermal fluctuations. It is very important to notice that the water states just below the Fermi energy belong to water molecules near the ends

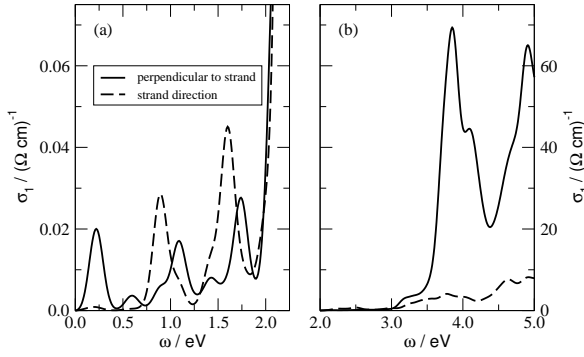


FIG. 2: Polarization dependence of the optical conductivity for a structure snapshot of a 5'-GAAT-3' sequence with Na counterions where  $\sigma_{1,\perp}(\omega)$  [ $\sigma_{1,\parallel}(\omega)$ ] is plotted with solid [dashed] lines. Panel (a) shows the low-energy features whereas panel (b) presents the range of the  $\pi-\pi^*$  transition. The theoretical line spectra are broadened with Gaussian functions of width 0.1 eV.

of the sequence [see panel (b) of Fig. 1]. Therefore, a small gap between HOMO and LUMO only appears if water molecules could enter the DNA structure on damage sites like ends, breaks, or nicks to contact the DNA bases.

The results of the projected DOS suggest the possibility of a thermally activated doping of the DNA by water states which should also lead to an electronic contribution to the low-frequency absorption. As one can see from panel (a) of Fig. 2, we indeed observe low-energy features in the optical conductivity. By studying the (fictitious) temperature dependence of these features within SIESTA, we can confirm that they are due to transitions between thermally occupied  $\pi^*$  states of the DNA bases. Furthermore, as you can see from panel (b), we also observe the well pronounced  $\pi-\pi^*$  transition at 3.8 eV. Whereas the polarization dependence of the low-energy absorption is rather small [see panel (a)] the in-plane  $\pi-\pi^*$  transition is much more visible if the electric field is perpendicular to the DNA strand direction. A less pronounced anisotropy of the optical conductivity has also been found in Ref. 11.

To take into account the dynamical character of the environment we average the results for the optical conductivity over up to 9 structure snapshots from the MD simulations. As discussed above, the low-energy features of the optical conductivity result from a doping of the DNA by water states. Therefore, they are strongly affected by environment fluctuations and we only obtain some smeared intensity in the low-energy range of the averaged conductivity. In contrast, the intrinsic  $\pi-\pi^*$  is much less effected by dynamical fluctuations so that we obtain well defined structures in that range.

Due to the intrinsic character of the  $\pi-\pi^*$  transition the averaged optical conductivity in the range between 2 eV and 5 eV is barely affected by the kind of counterions [see panel (a) of Fig. 3]. To show that the main structure

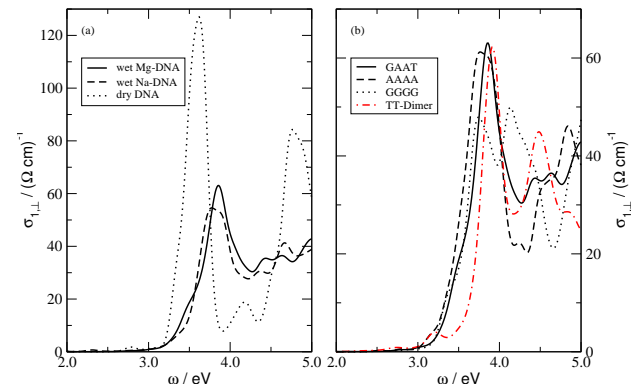


FIG. 3: Robustness of the  $\pi-\pi^*$  transition regarding environment and DNA sequence. Panel (a) shows the effects of the surrounding water molecules and counterions on the optical conductivity of a 5'-GAAT-3' sequence. The results for different B-DNA sequences in a wet environment containing Mg counterions are compared in panel (b). The spectra for the wet 5'-GAAT-3' (5'-AAAA-3', 5'-GGGG-3', and TT-dimer) sequences have been averaged over the results of 9 (5) structure snap shots. The theoretical line spectra are broadened with Gaussian functions of width 0.1 eV.

in the spectra around 3.7 eV really has to be interpreted as the intrabase  $\pi-\pi^*$  transition we also plot the optical conductivity of dry protonated B-DNA in panel (a) of Fig. 3. Although the spectra of wet and dry B-DNA considerably differ in the intensities, the peak positions agree quite well. Furthermore, as one can see from panel (b) of Fig. 3, peak position and shape of the  $\pi-\pi^*$  transition depend only weakly from the sequence whereas remarkable differences have been observed in the energy range between 4 eV and 5 eV.

*Discussion.* In Fig. 4 we compare our results with recent optical experiments [5] where we find a nice agreement for the range of the  $\pi-\pi^*$  transition above  $10000\text{ cm}^{-1}$ . However, we find a pronounced polarization dependence of the optical conductivity (see Fig. 2) whereas the experimental spectra are almost isotropic. This experimentally observed isotropic behavior can be explained by a substantial local direction variation of the macroscopically orientated DNA duplex [5].

The discussion of the spectra below  $500\text{ cm}^{-1}$  is more complicated because vibrational modes of the double helix structure and of the surrounding water molecules appear which are not included in our DFT calculations. In particular, the optical conductivity below  $100\text{ cm}^{-1}$  has been interpreted in Ref. 19 as a pure water dipole relaxation. However, our DFT calculations clearly show an electronic conductivity even at very low frequencies (see Fig. 4). As already discussed above, the low-frequency conductivity results from a doping of the DNA by water molecules near the bases. Therefore, the theoretically observed conductivity at low frequencies, which is approximatively one order of magnitude smaller than the

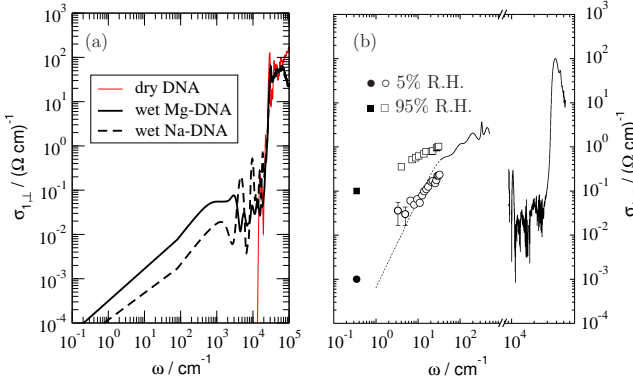


FIG. 4: Panel (a) is a log-log plot of the optical conductivity from Fig. 3, panel (a). Panel (b) shows experimental data for DNA in a 5% and 95% relative humidity environment taken from Ref. 5.

experimental values, would be further increased if more waters could enter the DNA structure on additional damage sites like ends, breaks, or nicks.

A striking aspect of the work of Briman *et al.* is the near identity of the microwave conductivity for single stranded and double stranded DNA [19]. This, as well as the order of magnitude discrepancy between our low frequency calculations and their data can possibly be resolved as follows: (i) We have order one water per tetramer associated with end bases; if this is upped to one level per base we gain a factor of eight in absorption intensity, close to that needed to resolve the discrepancy with the Briman *et al.* data. This is obviously plausible for single stranded DNA adsorbed to the sapphire substrate of Ref. 19. (ii) To get the same low frequency conductivity contribution for double stranded DNA as single stranded requires that the DNA flatten and unwind (the helix) as has been observed elsewhere for DNA on surfaces [20]. In the unwound configuration the extra space between bases allows for entry by water molecules. Obviously some of the microwave absorption will be caused by water motion alone as suggested by Ref. 19; our purpose here is to note that electronic absorption affiliated with defect states can be comparable.

One of the grand technological challenges of our times is to develop a rapid scheme for sequence differentiation in DNA, for example to be able to quickly differentiate between different alleles of a given gene. Current technologies, such as those of real-time or quantitative PCR, rely on fluorescent dyes and the FRET (Fluorescent Resonance Energy Transfer) method. This requires developing gene specific labeling dyes, or donors and ac-

ceptors, which will lead to fluorescent signals reflecting the amount of a given double-stranded DNA sequence in the system. However, the intrinsic electronic [22] as well as the optical properties of the DNA also vary from sequence to sequence. So, a natural question is: would it be possible some day to develop label-free optical fingerprinting of DNA that would allow one to infer different alleles directly from optical experiments without the use of dyes?

Optical fingerprinting would require two things to happen. First, one would need optical signatures predominantly from a given gene and one would need signals from different alleles to be sufficiently different. The former may be achieved by gene-chip and by surface enhancement techniques. We can address here the latter question, how different are the spectra from different sequences and consequently how easy would it be to establish such a difference experimentally. Clearly the spectra from different sequences strongly overlap and this makes it harder to distinguish them. Having large copies of the gene generated through polymerase chain reaction will lead to signal averaging and the time averaged signal can be distinguished if there is sufficient accuracy. For example, given the approximate 30% statistical variance for five configurations used in averaged conductivity calculations here for tetramers while the means diverge at the  $\approx 5\%$  level. Hence, we could expect single point frequency sampling to discern the sequences here with a configuration increase to 180. This number could likely be reduced with judicious use of multipoint frequency sampling. If a simple definitive fingerprint is required without full sequence information, as might be appropriate in applications in forensics or pathogen detection, numbers in the ballpark of 100-1000 clones of a given sequence could be sufficient. This compares with the  $10^5 - 10^6$  levels of clones necessary for current state of the art DNA sequencing technology[21]. Quantitative theoretical studies will be an important aid in developing such technologies.

We thank G. Grüner for the permission to use the plot of the experimental data from Ref. 5. This work was supported by NSF grant PHY 0120999 (the Center for Biophotonics Science and Technology) and DMR-0240918, by the US Department of Energy, Division of Materials Research, Office of Basic Energy Science, and by DFG grant HU 993/1-1. DLC is grateful for the support of the Center for Theoretical Biological Physics through NSF grants PHY0216576 and PHY0225630, and the J.S. Guggenheim Memorial Foundation.

[1] see, for example, C. Dekker and M.A. Ratner, Phys. World **14**, 29 (2001), and M. Di Ventra and M. Zwolak, in *Encyclopedia of Nanoscience and Nanotechnology*,

edited by H. Singh-Nalwa (American Scientific Publishers, 2004).

[2] E.M. Boon *et al.*, Proc. Nat. Acad. Sci. (USA) **100**, 12543

(2003).

- [3] R. G. Endres, D. L. Cox, and R. R. P. Singh, *Rev. Mod. Phys.* **76**, 195 (2004).
- [4] K.-H. Yoo *et al.*, *Phys. Rev. Lett.* **87**, 198102 (2001).
- [5] E. Helgren *et al.*, cond-mat/0111299.
- [6] C. R. Cantor and P. R. Schimmel, *Biophysical Chemistry: Part II*, W. H. Freeman Publishers (1980).
- [7] D. Sánchez-Portal *et al.*, *Int. J. Quantum Chem.* **65**, 453 (1997); E. Artacho *et al.*, *Phys. Status Solidi (b)* **215**, 809 (1999); P. Ordejón, E. Artacho, and J. M. Soler, *Phys. Rev. B* **53**, R10441 (1996).
- [8] R.N. Barnett *et al.*, *Science* **294**, 567 (2001).
- [9] A. Troisi and G. Orlandi, *J. Phys. Chem. B* **106**, 2093 (2002).
- [10] P. J. de Pablo *et al.*, *Phys. Rev. Lett.* **85**, 4992 (2000).
- [11] F. L. Gervasio, P. Carloni, and M. Parrinello, *Phys. Rev. Lett.* **89**, 108102 (2002).
- [12] R. G. Endres, D. L. Cox, and R. R. P. Singh, cond-mat/0201404.
- [13] J.P. Lewis *et al.*, *Phys. Stat. Sol. B* **233**, 90 (2002).
- [14] N. Troullier and J. L. Martins, *Phys. Rev. B* **43**, 1993 (1991).
- [15] L. Kleinman and D.M. Bylander, *Phys. Rev. Lett.* **48**, 1425 (1982).
- [16] J. P. Perdew, K. Burke, and M. Ernzerhof, *Phys. Rev. Lett.* **77**, 3865 (1996).
- [17] O. F. Sankey and D. J. Niklewski, *Phys. Rev. B* **40**, 3979 (1989).
- [18] D. A. Case *et al.*, AMBER 7, University of California, San Francisco (2002).
- [19] M. Briman *et al.*, *Nano Lett.* **4**, 733 (2004).
- [20] T. Kanno *et al.* *Appl. Phys. Lett.* **77**, 3848 (2000); L. Cai, H. Tabata, and T. Kawai, *Nanotechnology* **12**, 211 (2001).
- [21] J.C. Venter *et al.*, *Science* **280**, 1540 (1998).
- [22] M. Zwolak and M. Di Ventra, cond-mat/0411317.